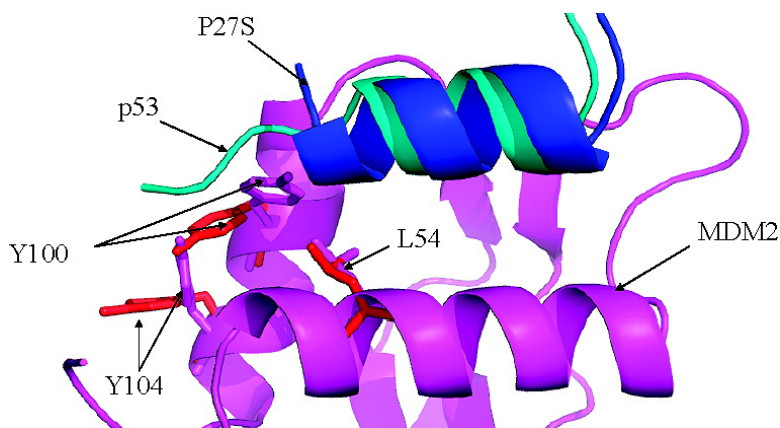


## Multiple Peptide Conformations Give Rise to Similar Binding Affinities: Molecular Simulations of p53-MDM2

Shubhra Ghosh Dastidar, David P. Lane, and Chandra S. Verma

*J. Am. Chem. Soc.*, **2008**, 130 (41), 13514-13515 • DOI: 10.1021/ja804289g • Publication Date (Web): 19 September 2008

Downloaded from <http://pubs.acs.org> on February 8, 2009



### More About This Article

Additional resources and features associated with this article are available within the HTML version:

- Supporting Information
- Links to the 1 articles that cite this article, as of the time of this article download
- Access to high resolution figures
- Links to articles and content related to this article
- Copyright permission to reproduce figures and/or text from this article

[View the Full Text HTML](#)



ACS Publications  
High quality. High impact.

## Multiple Peptide Conformations Give Rise to Similar Binding Affinities: Molecular Simulations of p53-MDM2

Shubhra Ghosh Dastidar,<sup>†</sup> David P. Lane,<sup>‡</sup> and Chandra S. Verma<sup>\*,†</sup>

Bioinformatics Institute (A-STAR), 30 Biopolis Street, #07-01 Matrix, Singapore 138671, and Institute of Molecular and Cell Biology (A-STAR), Proteos, 61 Biopolis Drive, Singapore 138673

Received June 12, 2008; E-mail: chandra@bii.a-star.edu.sg

The tumor suppressor activity of the transcription factor p53 is regulated by the E3-ubiquitin ligase MDM2.<sup>1</sup> Upon cellular stress, modifications such as phosphorylation disable the MDM2-p53 interaction. This stabilizes p53 in the cell which in turn induces cell cycle arrest, repair, and apoptosis. While 50% of human tumors harbor mutant p53, several contain wild type p53 and an overexpression of MDM2.<sup>1</sup> Disruption of the p53-MDM2 interaction between their N-terminal domains by peptides and small molecules stabilizes p53 leading to apoptosis *in vitro* and *in vivo* indicating possible therapeutic benefits.<sup>2–4</sup> Detailed molecular understanding of this interaction has emerged.<sup>5–7</sup> The crystal structure reveals the 19–25 region of the transactivation domain (TA) of p53 bound to the N-terminal domain of MDM2 as largely helical, with regions 17–18 and 26–29 unstructured.<sup>6</sup> Several lines of evidence prove unequivocally that residues F19, W23, and L26 are the three key p53 residues that are sequestered within, and important for, binding to MDM2 (Figure 1a). However neighboring residues also exert some influence.<sup>5,8</sup> But no detailed structural correlations have been reported.

In a recent study, Zondlo et al. demonstrated that the C-terminal end of the TA domain of p53 modulates binding to MDM2.<sup>9</sup> This led them to isolate several p53 peptide variants of which the W23L and P27S mutants displayed the lowest and highest affinities for MDM2, with binding free energies 3.0 and 2.3 kcal/mol weaker and stronger than wild type (WT) p53, respectively; P27S displayed the highest affinity among any peptide characterized so far. NMR experiments on the isolated peptide suggested that the replacement of P27 with S resulted in increased helicity, thus leading to tighter binding; however no atomic detail of the bound complex or the underlying mechanism was reported. We show, through molecular dynamics (MD) simulations, that mutual modulation of MDM2 and peptide conformations controls this variation.

We simulated the binding of WT, W23L, and P27S peptides to the N-terminal domain of MDM2. W23L was modeled based on the structure of WT, while, for P27S, we ran two simulations: one state (P27Sc) had the peptide modeled in the same conformation as that seen for WT, while the other (P27Sm) was modeled as a helix extending to the C-terminal, guided by NMR observations.<sup>9</sup> Molecular dynamics simulations and binding free energies were computed using the CHARMM22 force field for ~250 ns (see Supporting Information). The simulations were judged to be stable (Supporting Information Figure S1a); subtle changes in local and global dynamics characterize the different peptide complexes (Figure S1b, c). The secondary structure plots (Figure S2) show that the conformations of uncomplexed p53 and W23L are similar with no regular structure at the C-terminus, while P27Sm has a helical segment extending to L26; in contrast P27Sc is stabilized

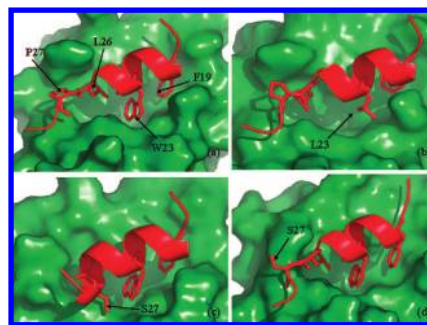


**Figure 1.** Snapshots taken at the end of 20 ns MD of (a) WT, (b) W23L, (c) P27Sm, and (d) P27Sc complexes.

as a  $\pi$ -helix with disorder at the C-terminus. Given that NMR shows P27S to be  $\alpha$ -helical, we use uncomplexed P27Sm for our analysis. In the complexed state, W23L shows somewhat reduced helicity; this is expected as the W  $\rightarrow$  L change leads to a loss of local interactions (Supporting Information movie M1).<sup>9</sup> Overall the behavior of complexed p53 is in agreement with previous reports<sup>10,11</sup> and is similar to complexed W23L. In contrast, P27Sm remains strongly helical from 19–28 in the complexed state, while P27Sc is helical only from 19–25 (same as WT and W23L). The N-terminal residues of P27S and W23L retain all the interactions with MDM2 as seen for WT including the important H-bond with Q72.<sup>8</sup> Additionally, in the MDM2-P27Sm complex we see some new H-bonds that stabilize the peptide helix: W23-S27, K24-E28, L25-N29.

In the WT, W23L, and P27Sc complexes, the P27 and the extended C-termini pack in a manner which keeps the Y100 (and Y104) pointing away from the MDM2 pocket, making an H-bond with E28 (Figures 1, 2 and movie M1). In contrast, in P27Sm, the S27 side chain and the rest of the C-terminus are now part of the turn of a helix, shortening the peptide length and creating a cavity in the space occupied by the extended C-terminus, most notably by P27. This results in reorientation of Y100 (and Y104 in concert; see Figures 2 and S3 and movie M1) toward the MDM2 pocket as it now forms an H-bond with the L26 backbone. It further packs against L54 and results in a more compact binding pocket and, together with reorientation of H96, leads to a “cozier” fitting of the peptide. L54 and Y100 together act like a “gate” (Figure 2) to increase or decrease the size of the binding pocket, which seems to be modulated by the nature of the peptide/ligand that occupies the MDM2 cavity;<sup>12</sup> there is no evidence for this flip in the uncomplexed MDM2 (Figure S3). Indeed, similar orientations of Y100 are seen in crystal structures of several MDM2 complexes (Figure S4); in some cases, Y104 points away due to crystal contacts (in unpublished simulations, it undergoes flipping). In the structure of p53 complexed to homologue MDMX, equivalent Y96 is reoriented despite the presence of P27;<sup>13</sup> however the p53 peptide

<sup>†</sup> Bioinformatics Institute; C.S.V. is adjunct at DBS (NUS); SBS (NTU).

<sup>‡</sup> Institute of Molecular and Cell Biology.

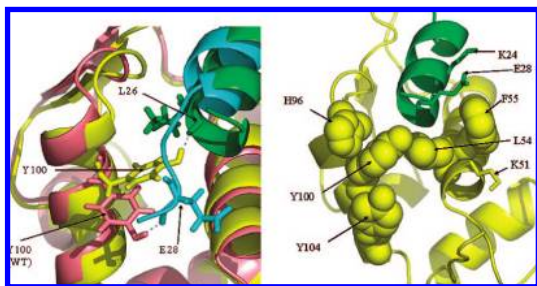


**Figure 2.** (Left) Superimposed complexes: WT MDM2 (salmon red)-p53 (cyan) and MDM2 (yellow)-P27Sm (green), showing Y100 orientations. (Right) reoriented MDM2 residues forming a “gate” leading to “cozies” fit of peptide (also see Supporting Information).

**Table 1.** Binding Free Energy (kcal/mol) and Components for Different Peptides (Also See Supporting Information)<sup>9</sup>

$\Delta(\text{binding})$	W23L	p53	P27Sm	P27Sc
$E_{\text{mm}} (\Delta H)$	-51.4	-54.7	-58.3	-55.5
$-T\Delta S$	39.3	38.4	37.3	35.0
$\Delta G$	-12.1	-16.3	-21.0	-20.5
$\Delta\Delta G$	4.2	0.0	-4.7	-4.2
$\Delta G (\text{expt})^a$	-6.0	-9.0		-11.3
$\Delta\Delta G (\text{expt})^a$	3.0	0.0		-2.3

<sup>a</sup> Experimental data (error in  $\Delta\Delta G \sim 0.4$  kcal/mol).

is terminated at P27 and lacks the C-terminal extension that packs it against the surface of MDM2. The importance of L54, H96, and Y100 had also been highlighted by *in silico* mutagenesis.<sup>10</sup> The helical conformation at the C-terminus of P27Sm also brings E28 of the peptide close to K24 (3.7Å), resulting in a new salt bridge that further stabilizes the helical conformation; in contrast, in the other systems these two residues are  $\sim 11$  Å apart (see Figure S5).

The computed free energy differences ( $\Delta G$ ) between W23L and p53 and between p53 and P27S are very similar to experimental values (Table 1); similar trends have been reported in other studies (extensive conformations of the various states are elaborated upon in the Supporting Information).<sup>8,10,11</sup> Unbound P27S has been taken to be helical (P27Sm) as has been determined experimentally, while its complexed state was either helical (as guided by NMR) or extended at the C-terminus (as guided by the WT structure). Surprisingly, in both cases,  $\Delta G_{\text{bind}}$  is similar ( $-21.0$  or  $-20.5$  kcal/mol); however while P27Sm has the enthalpic advantage, P27Sc has an entropic advantage. The loss of binding of W23L originates in a destabilized enthalpy, largely due to the loss of packing and of an H-bond between the side chain NH of W23 and the backbone CO of L54 (this leads to a loss of  $\sim 4$  kcal of enthalpy as would be expected for a good H-bond). In a similar study, the W23A mutation incurred a 6.3 kcal/mol loss.<sup>8</sup> The burial of the NH of W23 incurs a large desolvation penalty (Table S2). In W23L, packing of W23 and L26 is lost, leading to a larger entropic penalty. In P27Sm, the packing of P27 against the MDM2 surface is lost, leading to destabilized van der Waals interactions which is offset by electrostatic stability arising from increased polarity and the formation of intrapeptide H-bonds; the larger helicity of P27Sm also results in a smaller entropic penalty upon complex formation. P27Sc undergoes a small enthalpic gain relative to WT and large entropic gain (3.4 kcal/mol) as the Pro  $\rightarrow$  Ser change increases the flexibility in the complex. P27Sc undergoes a helical  $\rightarrow$  extended transition while P27Sm undergoes a helical  $\rightarrow$  helical transition, thus accounting for a larger entropic cost for the latter. However both of these are more favorable than WT and W23L which undergo an extended  $\rightarrow$  extended transition.

Molecular dynamics simulations, guided by experimental information<sup>9</sup> have successfully reproduced experimental trends in binding affinities of mutant p53 peptides with MDM2. Simulations reveal the following: (a) higher helicity of the peptide leads to greater affinity as postulated experimentally; additionally the surface of MDM2 adapts optimally to bind various peptide/ligands as has been postulated;<sup>14–18</sup> (b) the uncomplexed peptides are governed by a combination of helicity and intrinsic disorder (in agreement with experiments), while in the complexed state two very different conformations can coexist. This yields very similar binding affinities, driven by either enthalpy or entropy. Y100 is highly conserved (Figure S6) and acts as a gate whose orientations discriminate between the two types of peptide conformations and provides a new parameter to take into account in the design of new peptidic and small molecule inhibitors.<sup>12</sup> The importance of the adaptive surface of MDM2 for drug design is underscored by our observations.<sup>19</sup> The altered structure of the MDM2 surface leads to characteristic differences in electrostatic potentials (Figure S7) that we are currently using to design new peptides. In summary, we show for the first time how the ensemble of a protein–peptide complex seems to originate in conformational diversity leading to higher affinity (also see Supporting Information).

**Acknowledgment.** This work was supported by the Biomedical Research Council (Agency for Science, Technology and Research), Singapore. We thank Sebastian Maurer-Stroh and Janos Kriston-Vizi for technical help and Prof. Tad Holak for making available the new MDMX-p53 structure.

**Supporting Information Available:** Simulated structures are available upon request from the authors. Details of the simulation and movies are available as Supporting Information. This material is available free of charge via the Internet at <http://pubs.acs.org>.

## References

- (1) Vogelstein, B.; Lane, D.; Levine, A. J. *Nature* **2000**, *408*, 307–310.
- (2) Bottger, A.; Bottger, V.; Sparks, A.; Liu, W. L.; Howard, S. F.; Lane, D. P. *Curr. Biol.* **1997**, *7*, 860–869.
- (3) Vassilev, L. T.; Vu, B. T.; Graves, B.; Carvajal, D.; Podlaski, F.; Filipovic, Z.; Kong, N.; Kammlott, U.; Lukacs, C.; Klein, C.; Fotouhi, N.; Liu, E. A. *Science* **2004**, *303*, 844–848.
- (4) Dey, A.; Verma, C. S.; Lane, D. P. *Br. J. Cancer* **2008**, *98*, 4–8.
- (5) Bottger, A.; Bottger, V.; Garcia-Echeverria, C.; Chene, P.; Hochkeppel, H. K.; Sampson, W.; Ang, K.; Howard, S. F.; Pickles, S. M.; Lane, D. P. *J. Mol. Biol.* **1997**, *269*, 744–756.
- (6) Kussie, P. H.; Gorina, S.; Marechal, V.; Elenbaas, B.; Moreau, J.; Levine, A. J.; Pavletich, N. P. *Science* **1996**, *274*, 948–953.
- (7) Lee, H.; Mok, K. H.; Muhandiram, R.; Park, K. H.; Suk, J. E.; Kim, D. H.; Chang, J.; Sung, Y. C.; Choi, K. Y.; Han, K. H. *J. Biol. Chem.* **2000**, *275*, 29426–29432.
- (8) Massova, I.; Kollman, P. A. *J. Am. Chem. Soc.* **1999**, *121*, 8133–8143.
- (9) Zondlo, S. C.; Lee, A. E.; Zondlo, N. J. *Biochemistry* **2006**, *45*, 11945–11957.
- (10) Zhong, H.; Carlson, H. A. *Proteins* **2005**, *58*, 222–234.
- (11) Lee, H. J.; Srinivasan, D.; Coomber, D.; Lane, D. P.; Verma, C. S. *Cell Cycle* **2007**, *6*, 2604–2611.
- (12) Buolamwini, J. K.; Addo, J.; Kamath, S.; Patil, S.; Mason, M.; Ores, M. *Curr. Cancer Drug Targets* **2005**, *5*, 57–68.
- (13) Popowicz, G. M.; Czama, A.; Rothweiler, U.; Szwagierczak, A.; Krajewski, M.; Weber, L.; Holak, T. A. *Cell Cycle* **2007**, *6*, 2386–2392.
- (14) Espinoza-Fonseca, L. M.; Trujillo-Ferrara, J. G. *Biopolymers* **2006**, *83*, 365–373.
- (15) Uhrinova, S.; Uhrin, D.; Powers, H.; Watt, K.; Zheleva, D.; Fischer, P.; McInnes, C.; Barlow, P. N. *J. Mol. Biol.* **2005**, *350*, 587–598.
- (16) Schon, O.; Friedler, A.; Bycroft, M.; Freund, S. M.; Fersht, A. R. *J. Mol. Biol.* **2002**, *323*, 491–501.
- (17) Showalter, S. A.; Bruschweiler-Li, L.; Johnson, E.; Zhang, F.; Bruschweiler, R. *J. Am. Chem. Soc.* **2008**, *130*, 6472–6478.
- (18) Chen, H.-F.; Luo, R. *J. Am. Chem. Soc.* **2007**, *129*, 2930–2937.
- (19) Bowman, A. L.; Nikolovska-Coleska, Z.; Zhong, H.; Wang, S.; Carlson, H. A. *J. Am. Chem. Soc.* **2007**, *129*, 12809–12814.

JA804289G